Genes & Diseases (2022) 9, 1086–1098

Available online at www.sciencedirect.com

ScienceDirect

journal homepage: http://ees.elsevier.com/gendis/default.asp

FULL LENGTH ARTICLE

Downregulation of *nc886* contributes to prostate cancer cell invasion and TGFβ1-induced EMT

Ronghui Yang [a,1], Lingkun Zuo [a,1], Hui Ma [a], Ying Zhou [a], Ping Zhou [b], Liyong Wang [a], Miao Wang [c], Mahrukh Latif [d], Lu Kong [a,*]

[a] *Department of Biochemistry and Molecular Biology, Capital Medical University, Beijing 100069, PR China*
[b] *Biomedical Engineering Institute of Capital Medical University, Capital Medical University, Beijing 100069, PR China*
[c] *Department of Pathology, Beijing Friendship Hospital, The Second Clinical Medical College of Capital Medical University, Beijing 100050, PR China*
[d] *Department of Nuclear Medicine, Fourth Hospital of Hebei Medical University, Shijiazhuang, Hebei 050010, PR China*

Received 22 June 2020; received in revised form 9 December 2020; accepted 24 December 2020
Available online 9 February 2021

KEYWORDS
EMT;
MET;
Non-coding RNA;
Prostate cancer;
TGF-β1

Abstract Epithelial-to-mesenchymal transition (EMT) activation is important in cancer progression and metastasis. Evidence indicates that *nc886* is a representative Pol III gene that processes microRNA products via Dicer and further downregulates its target gene transforming growth factor- β1 (TGF-β1), which is the most prominent inducer of EMT in prostate cancer (PC). Consistent with the previous literature, we found that *nc886* downregulation was strongly associated with metastatic behavior and showed worse outcomes in PC patients. However, little is known about the association between *nc886* and the EMT signaling pathway. We developed a PC cell model with stable overexpression of *nc886* and found that *nc886* changed cellular morphology and drove MET. The underlying mechanism may be related to its promotion of SNAIL protein degradation via ubiquitination, but not to its neighboring genes, TGFβ-induced protein (*TGFBI*) and *SMAD5*, which are Pol II-transcribed. TGF-β1 also override nc886 promotion of MET via transient suppression the transcription of *nc886*, promotion of *TGFBI* or increase in SMAD5 phosphorylation. Both *nc886* inhibition and *TGFBI* activation occur regardless of their methylation status. The literature suggests that MYC inhibition by TGF-β1 is attributed to *nc886* downregulation. We incidentally identified MYC-associated zinc finger

* Corresponding author.
E-mail address: konglu@ccmu.edu.cn (L. Kong).
Peer review under responsibility of Chongqing Medical University.
[1] These authors have contributed equally to this work.

https://doi.org/10.1016/j.gendis.2020.12.010
2352-3042/Copyright © 2021, Chongqing Medical University. Production and hosting by Elsevier B.V. This is an open access article under the CC BY-NC-ND license (http://creativecommons.org/licenses/by-nc-nd/4.0/).

protein (MAZ) as a suppressive transcription factor of TGFBI, which is controlled by TGF-β1. We elucidate a new mechanism of TGF-β1 differential control of Pol II and the transcription of its neighboring Pol III gene and identify a new EMT unit consisting of *nc886* and its neighboring genes.

Copyright © 2021, Chongqing Medical University. Production and hosting by Elsevier B.V. This is an open access article under the CC BY-NC-ND license (http://creativecommons.org/licenses/by-nc-nd/4.0/).

Introduction

Prostate cancer (PC) is common in older men. Prostate-specific antigen-based screening is controversial in reducing the mortality of PC.[1] Therefore, the identification of surrogate biomarkers associated with advanced or metastatic PC requires more effort.

Current discoveries and advances in the use of ncRNAs as biomarkers have clinical implications in PC.[2] *Nc886* (pre-miR-886, CBL3, or VtRNA2-1) was recently identified as a new type of noncoding RNA.[3] The *nc886* gene, which is located near a differentially methylated region (DMR) of human chromosome 5, is imprinted and may show allele-specific expression.[4] This gene and its microRNA products (hsa-miR-886-3p and -5p) are often hypermethylated and suppressed in a wide range of cancers, such as cholangiocarcinoma,[5] acute myeloid leukemia (AML),[6] and esophageal,[7] gastric,[7] and lung[8] tumors, and it plays a putative tumor-suppressive role via direct inhibition of protein kinase R.[9] However, levels of *nc886* and its microRNA are upregulated in some cancers, including human familial non-medullary thyroid cancer,[10] clear cell renal cell carcinoma,[11] endometrial cancer,[12] high-grade and invasive bladder tumors,[13] and cervical cancer,[14] which suggests an oncogenic role. Therefore, its precise role in cancer requires further confirmation.

Fort et al[15,16] suggested that *nc886* and its microRNA (also *snc886-3p* or *-5p*) processed by Dicer have clinical importance in advanced or metastatic PC, and its expression is silenced by methylation in metastases, which increases cell proliferation and invasive ability. *Snc886-3p* assists its precursor *nc886* in the suppression of tumor growth and invasion in PC primarily due to its target genes, which are associated with cancer cell proliferation and progression. TGF-β1 is a direct target of hsa-miR-886-3p, and it was suppressed at posttranscriptional levels in small cell lung cancer.[8] Our previous transcriptome sequencing data also suggested that *nc886* downregulated *TGFB1* mRNA in highly metastatic PC cell lines.[17] Lee YS et al demonstrated that TGF-β induced the expression of *nc886*, and *nc886* emulated TGF-β to promote ovarian cancer progression.[18] These data support a mutual regulation between *nc886* and TGF-β1.

TGF-β1 is generally well characterized in PC initiation and progression, and it induces EMT in PC cells.[19] EMT refers to the process by which the expression of mesenchymal markers (such as vimentin and N-cadherin) prevails over epithelial markers (such as E-cadherin) in the balance.[20] EMT transcription factors (EMT-TFs), SNAIL, SLUG and TWIST downregulate E-cadherin level and change cell plasticity via binding to the E-boxes of the *CDH1* promoter in PC.[21,22] EMT endows cells with migratory and invasive properties to orchestrate the initiation of metastasis.[23] Notably, we observed that stable *nc886*-overexpressing PC cell lines exhibited epithelial-like characteristics with lower invasive ability in our model. TGF-β1 may be a core signal in linking *nc886* with PC. Therefore, the present research elucidates the underlying molecular mechanism of the contribution of *nc886* epigenetic silencing to PC invasion and its correlation with the TGF-β-induced EMT pathway, which was rarely reported.

TGFBI (a TGF-β-induced gene) and *SMAD5* are effectors in TGF-β-mediated EMT and border *nc886*. TGFBI-induced EMT accelerates the metastasis of PC.[24] However, early contradictory research suggested that promoter methylation regulates the function of TGFBI as a tumor suppressor in PC and lung cancer.[25] Hypermethylation of the *TGFBI* promoter is often associated with malignancies.[26] Our bioinformatic analysis revealed that high *TGFBI* expression was associated with higher PC Gleason grade and negatively correlated with its promotor methylation. However, there was a decrease in PC metastases (Fig. S2). High TGFBI expression indicated a mesenchymal state of tumors, not cancer progression.[27] These data suggest a common epigenetic modification, i.e., methylation, between *nc886* and *TGFBI*. *SMAD5* expression in PC positively correlated to *TGFBI* in our analysis, but negatively correlated to *nc886* (Fig. S2). Phosphorylated SMAD1/5 are transcript factors and active mediators in the TGF-β-induced EMT process.[28] Lee YS et al showed that TGF-β induced all of the three neighboring genes in the ovary cancer cell line SKOV3, but *SMAD5* expression was weaker than *TGFBI* and *nc886*.[18] We propose that the three adjacent genes functionally constitute an EMT-synergistic unit regulated by TGF-β, which may play a key role in PC invasion and metastasis. The underlying molecular mechanisms must be elucidated.

Materials and methods

Cell culture and reagents

Human cervical cancer cell lines HeLa and SiHa, the human prostate cancer cell line Du145 and urinary bladder carcinoma (T24) cells were purchased from the Chinese Academy of Science Cell Bank (Shanghai, China). The highly metastatic human PC epithelial cell line PC-3M-1E8 (1E8) and the low metastatic line PC-3M-2B4 (2B4) were obtained from the Peking University Health Science Center (Beijing, China). HeLa, SiHa and Du145 cells exhibit higher *nc886* expression

than in T24, 1E8 and 2B4 cells. Recombinant human TGFβ1 was purchased from PeproTech (96-100-21-10, CT, USA). Cells were incubated in serum-free medium overnight then treated with TGFβ1 for the indicated times. Cells were treated with different concentrations of 5-aza-2′-deoxycytidine (A3656, Sigma) for 5 days and DMSO or Mock as a control by replacing the medium with freshly added drug every 24 h, following the manufacturer's instructions.

Chromatin immunoprecipitation (ChIP)

ChIP experiments were performed following the protocol of the EZ-Magna ChIP assay kit (17—10086, Millipore). One microgram of anti-Pol II was used as a positive control, and the same amount of normal rabbit IgG was used as a negative control. One percent of input and 10% of the immune precipitates were used in PCR analyses using Taq 2 × PCR Master Mix (TQ2201-01, Omega) for 30 cycles at 95 °C for 30 s, 58 °C for 30 s, and 72 °C for 60 s. The primers used for ChIP are listed in the Supplementary Table.

RNA immunoprecipitation (RIP) assay

All RIP experiments were performed per the instructions of the RIP-Assay Kit (No. RN1001, MBL, Japan). Anti-DUBA3 (17802-1-AP, Proteintech) or SNAIL antibody (#3879, CST) was used to pull down endogenous nc886 complexes in 1E8 cells (1×10^8 cells). Details are provided in the Supplementary Materials and Methods.

Oligonucleotide synthesis and plasmid preparation

The pGLV3-overexpressing *nc886* plasmids and negative control plasmids were ordered from Shanghai GenePharma (Shanghai, China). We customized *nc886* mimics from Invitrogen (Carlsbad, CA, USA). All sequence information is provided in the Supplementary Table.

Lipofectamine RNAiMax reagent (Invitrogen) was prepared for cell transfection. A total of 1×10^6 cells in a 6-well plate were transfected with 50 nM oligonucleotides or 2 μg of plasmid. To acquire stable *nc886*-overexpressing 1E8 cell lines, mimic plasmids or control plasmids were transfected and selected in the presence of puromycin (Sigma, Merck Life Science, Shanghai, China).

Pyrosequencing of the *nc886* or TGFBI promoter

The methylation status of eight CpG islands in the nc886 promoter or 11 CpG islands in the *TGFBI* promoter was measured using pyrosequencing. Genomic DNA was extracted using a DNA Purification Kit (No. A1120, Promega, USA). One microgram of DNA was used for bisulfite conversion using an EpiTect® Bisulfite DNA Methylation Kit (No. 59104, QIAGEN, CA, USA). Fifty nanograms of converted DNA were amplified using touchdown PCR. The forward primer was labeled with biotin. Therefore, the PCR products were biotinylated and purified using streptavidin-Sepharose beads (GE Healthcare, USA). After sequencing in the PyroMark ID system (QIAGEN, Germantown, MD, USA), the results were analyzed using PyroMark software (Q24 2.0.6, QIAGEN). Primer sequences are provided in the Supplementary Table. Pyrosequencing assays were repeated 2 times, and the methylation level for each individual CpG site was averaged.

BALB/c nude mouse bone metastasis model and bone marrow (BM) isolation

Five-week-old male nude mice (animal ethics number AEEI-2018-067) were used to investigate tumor metastasis. A total of 1×10^5 1E8 cells with stable *nc886* overexpression or control vector were injected into the left ventricle of mice after anesthesia. Each group included at least 10 mice. The animals were sacrificed humanely 4 weeks after tumor cell injection. BM cells were isolated by pelleting and suspended in DMEM containing 10% fetal bovine serum. After overnight culture at 37 °C, suspended cells were discarded, and adherent cells were preserved in new DMEM. Cell morphology was photographed under an inverted fluorescence microscope. The tumors were confirmed by histological examination.

Ubiquitination assay

Control and mimic cells were lysed in RIPA buffer (P0013B) after incubation with 10 μM MG132 for 6 h. The supernatants were precleared using Protein A/G PLUS-Agarose (sc-2003) at 4 °C with rotation for 30 min. One milliliter of 300 μg/mL total cellular protein was transferred and added to 1 μg of anti-SNAIL (#3879, CST) at 4 °C with rotation for 2 h. Agarose beads (50 μL) were added to the sample and rotated overnight at 4 °C. Immunoprecipitants were transferred and washed 4 times with 1 mL of RIPA buffer. After the final washing, 50 μL of loading buffer was pipetted into the sample and boiled for 5 min at 95 °C for SDS-PAGE analysis.

Statistical analysis

SPSS 19.0 software (Chicago, IL, USA) and GraphPad 5.0 software (San Diego, CA, USA) were used for statistical analyses. Student's *t*-test and the nonparametric Spearman rank-correlation test were used in our proposal. All the tests were two-tailed, and statistically significant values were set at $P < 0.05$. At least three independent datasets were summarized and averaged.

Results

Nc886 is epigenetically suppressed in PC tissues and various cancer cells

Graded ISH results demonstrated a lower tendency of *nc886* expression in high-Gleason (GS, $N = 15$) and low-GS PC tissues ($N = 10$) than adjacent normal tissues ($N = 5$) (Fig. 1A, B). However, no statistical significance was observed due to the small sample size as a limitation. Fort et al (2018) investigated the *nc886* TSS200 methylation status in the TCGA-PRAD cohort and showed correlations with tumor metastasis and Gleason grade.[15] This group recently demonstrated that *nc886* produced two microRNAs, namely *snc886-3p* and *-5p*, which are processed by DICER, and

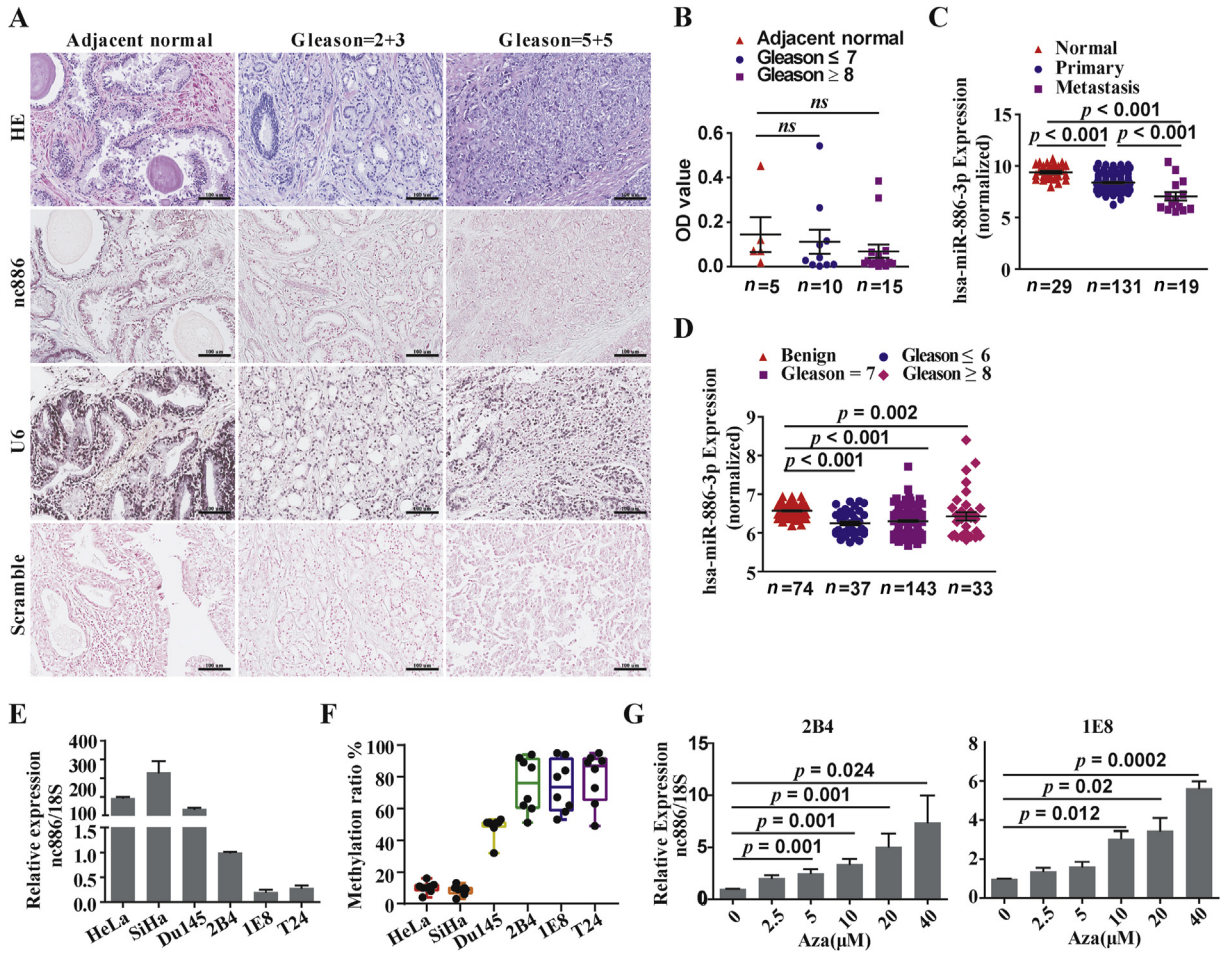

Figure 1 Low *nc886* or *snc886-3p* expression is associated with promoter methylation and PC metastasis event. The expression levels of *nc886* were examined using ISH in tissue arrays. **(A)** A 3′-DIG-labeled nc886 LNA probe, snRNA U6 (positive control), and scramble (negative control) were used. H&E staining suggested PC tissue GS grade (×200). Representative ISH images (×200) from low-GS or high-GS PC tissues showed weaker staining than the adjacent normal tissue. All images were acquired using an Aperio ImageScope system. **(B)** Statistical graph showing *nc886* expression in tissue assays, 5 adjacent normal tissues, 10 low or intermediate GS (≤7) tumors, and 10 high-GS (≥8) tumors relative to U6; nonparametric tests. **(C, D)** Hsa-miR-886-3p *(snc886-3p)* expression data (log_2-normalization) were extracted and analyzed from the publicly available GEO datasets GSE21032 (PC metastasis cohort) and GSE70770 (PC different GS grade cohort). **(E)** RT-qPCR quality analysis of the nc886 expression in 6 cell lines showing negative expression in 2B4, 1E8 and T24 cells and high expression in HeLa, SiHa and Du145 cells. **(F)** Quality plot for *nc886* average promoter methylation using pyrosequencing showing a total of 8 CpG sites in the 6 cell lines. **(G)** Expression of nc886 in 1E8 and 2B4 cells stimulated with different concentrations of 5-Aza-dC relative to untreated cells. Two-tailed Student's *t*-test. $P < 0.05$ indicated a significant difference. The data shown represent the means ± SD of at least 3 independent experiments.

snc886-3p was a tumor suppressor in PC cells.[16] Therefore, we considered the available *sn886-3p* expression data in public databases as a better proxy for *nc886* expression. We observed that metastatic tumors exhibited the lower levels of *snc886-3p* than primary tumors and normal tissues, as shown in the GSE21032 data (Fig. 1C). *Nc886* promoter methylation negatively correlated with its expression using Spearman correlation analysis (*P*-value = 0.023, Fig. S1A). Findings from the GSE70770 cohorts also revealed lower levels of *snc886-3p* in different Gleason groups than benign tissues (Fig. 1D). These data are consistent with the Fort RS report.[15,16]

Pyrosequencing data also demonstrated that the *nc886* DNA hypermethylation was accompanied by low expression in 6 cell lines (Fig. 1E, F, S4B). Sequencing primer information, bisulfite conversion PCR products and detailed methylation information are shown in Figure S1B and Figure S3B. The 2B4 and 1E8 cell lines were treated with the DNA methylation inhibitor 5-aza-2′-deoxycytidine (5-Aza-dC), which effectively induced the re-expression of *nc886* in a dose-dependent manner (Fig. 1G). We confirmed that *nc886* was suppressed due to CpG DNA hypermethylation in PC tissues and cells, and methylation correlated with cancer progression and metastasis.

Nc886 reduces the tumor aggression of PC cells, which is reversed by TGF-β1

To examine the real function of *nc886* in tumor metastasis, we constructed a cell model of *nc886* stable overexpression (hereafter referred to as "mimic" or "1E8^{nc886+}") in a 1E8 cell line with high invasive ability (Fig. 2A). Notably, the mimic changed its cancer cellular morphology and exhibited epithelial characteristics, which consisted of higher expression of E-cadherin or β-catenin and lower expression of N-cadherin, SNAIL or SLUG relative to the control group (Fig. 2B), which may be an important mechanism of *nc886* promotion of colony formation. The mimic group exhibited increased colony formation (Fig. 2C) but decreased migration and invasive ability (Fig. 2E, F) under nc886 overexpression to an approximately 1000-fold level of the negative control (Fig. 2A). Notably, 10 ng/mL TGF-β1 significantly promoted the invasive ability of control and mimic cells (Fig. 2F). However, nc886 overexpression did not affect cell proliferation (Fig. 2D).

In vivo, 1×10^5 cancer cells were injected into the left ventricles of BALB/c nude mice to investigate the differences between mimic and control cells in distant metastatic ability after 28 days. We observed a large number of GFP-positive cancer cells from BM aspirates in the control group but not in the mimic group (Fig. 2G). Clearly, *nc886* decreased the aggressive ability of tumor cells. However, its mechanism was not clear. Unfortunately, we failed to generate an nc886-KO HeLa or Du145 cell model because of cell growth retardation using CRISPR-Cas9 techniques (Supplementary Materials and Methods), which suggests that *nc886* is a lethal gene. Some evidence shows that *nc886* silencing activates PKR and induces apoptosis as one such mechanism.[29,30]

Nc886 reverses EMT features likely via the promotion of SNAIL ubiquitination

Nc886, which is transcribed in an antisense direction, is adjacent to two important genes in the EMT signaling pathway. One gene is the *TGFBI* gene, which is positioned head-to-head and may be a key mesenchymal subtype signature molecule, and the other gene is *SMAD5*, which has a tail-to-tail position in relation to *nc886* (Fig. 3A). We asked whether *nc886* promoted MET via *TGFBI* or *SMAD5*. *Nc886* had no effect on the expression of *SMAD5* or *TGFBI* mRNA or protein using RT-qPCR or Western blot assays, respectively, in mimic cells (Fig. 3B) or nc886-KO HeLa cells (Fig. 3C), which suggests that *nc886* did not directly regulate its neighboring genes *SMAD5* or *TGFBI* and that neither *TGFBI* nor *SMAD5* caused this epithelial subtype in the mimic group. Regrettably, nc886-KO HeLa cells failed to proliferate, and Western blot was not performed.

SNAIL protein expression was downregulated approximately 7-fold in mimic cells (Fig. 2B). SNAIL is a suppressive transcription factor for E-cadherin. *CDH1* mRNA was upregulated approximately 2-fold in mimic cells (Fig. 3D). Therefore, *nc886* may increase the protein level of E-cadherin directly via the downregulation of SNAIL expression. However, *SNAIL1* mRNA showed no changes with 24-h transient or stable overexpression of *nc886* (Fig. 3E), which suggests that SNAIL is regulated post-translationally. We observed SNAIL protein re-expression in mimic cells after treatment with the proteasome inhibitor MG132 but not with an inhibitor of autophagy and toll-like receptors (Fig. 3F), chloroquine, which confirmed that SNAIL expression was regulated post-translationally via the ubiquitin-proteasome system (UPS). *Nc886* obviously increased the ubiquitination levels of endogenous SNAIL protein (Fig. 3G) in IP experiments after MG132 treatment for 12 h. The SNAIL antibody successfully pulled down the *nc886* sequence using PCR detection, but the DUBA3 (a deubiquitinating enzyme) antibody did not pull down the sequence in the subsequent RIP experiment. These results suggest an interaction between *nc886* and SNAIL protein (Fig. 3H).

The bioinformatics analysis also suggested that *nc886* expression positively correlated with *CDH2* and *CTNNB1* but negatively correlated with *CDH1* and *SMAD5* based on GSE70770 data, which is contradictory to the results of the *in vitro* experiments. This discrepancy may be caused by the inconsistency between mRNA and protein levels or the more complicated EMT in tissue samples. These results require further validation in clinical samples.

The expression changes of *nc886* and its neighboring genes in TGF-β1-induced EMT process

To confirm that the rescue of TGF-β1 promoted 1E8^{nc886+} cell migration and invasion in Transwell experiments, we examined cell morphological and EMT molecule changes in 1E8^{nc886+} cells compared to controls following TGF-β1 stimulation for 5 days. The results showed that 1E8^{nc886+} and control cells exhibited an elongated fibroblast-like morphology after 5 days (Fig. 4A). Western blot analysis showed a significant reduction in E-cadherin in 1E8^{nc886+} cells and an increase in N-cadherin in the control group after stimulation with 15 or 20 ng/mL TGF-β1 for 5 days (Fig. 4B). These findings indicated that high-concentration and long-term TGF-β1 stimulation sufficiently induced EMT progression and restored mesenchymal characteristics in 1E8^{nc886+} cells. SNAIL was also slightly increased in 1E8^{nc886+} cells after TGF-β1 stimulation, which partially involved the downregulation of E-cadherin in 1E8^{nc886+} cells. We investigated the TGF-β1-induced changes in *nc886*, *TGFBI*, *SMAD5* and other EMT markers in mimic cell models. *Nc886* expression was downregulated, but *TGFBI* expression was much more upregulated (by 5-fold) in the control group and mimic group following induction by 10 ng/mL TGF-β1 for 2 h, with no observed effect on *SMAD5* expression (Fig. 4C, as shown by qRT-PCR). These data were subsequently validated at the protein level using ELISA for TGFBI (Fig. 4D). TGF-β1 temporarily decreased the expression of *nc886* in a concentration-dependent manner in mimic cell models (Fig. 4E). We also found that TGF-β1 temporarily and commonly reduced *nc886* expression in a time- and concentration-dependent manner for 1 h in *nc886*-expressing cells (Fig. 4F). TGF-β1 did not induce *nc886* expression in *nc886*-negative cells. Considering the short half-life of *nc886* (approximately 75 min), we speculated that TGF-β1 inhibits *nc886* expression within a short time. We also observed that TGF-β1 intensely and

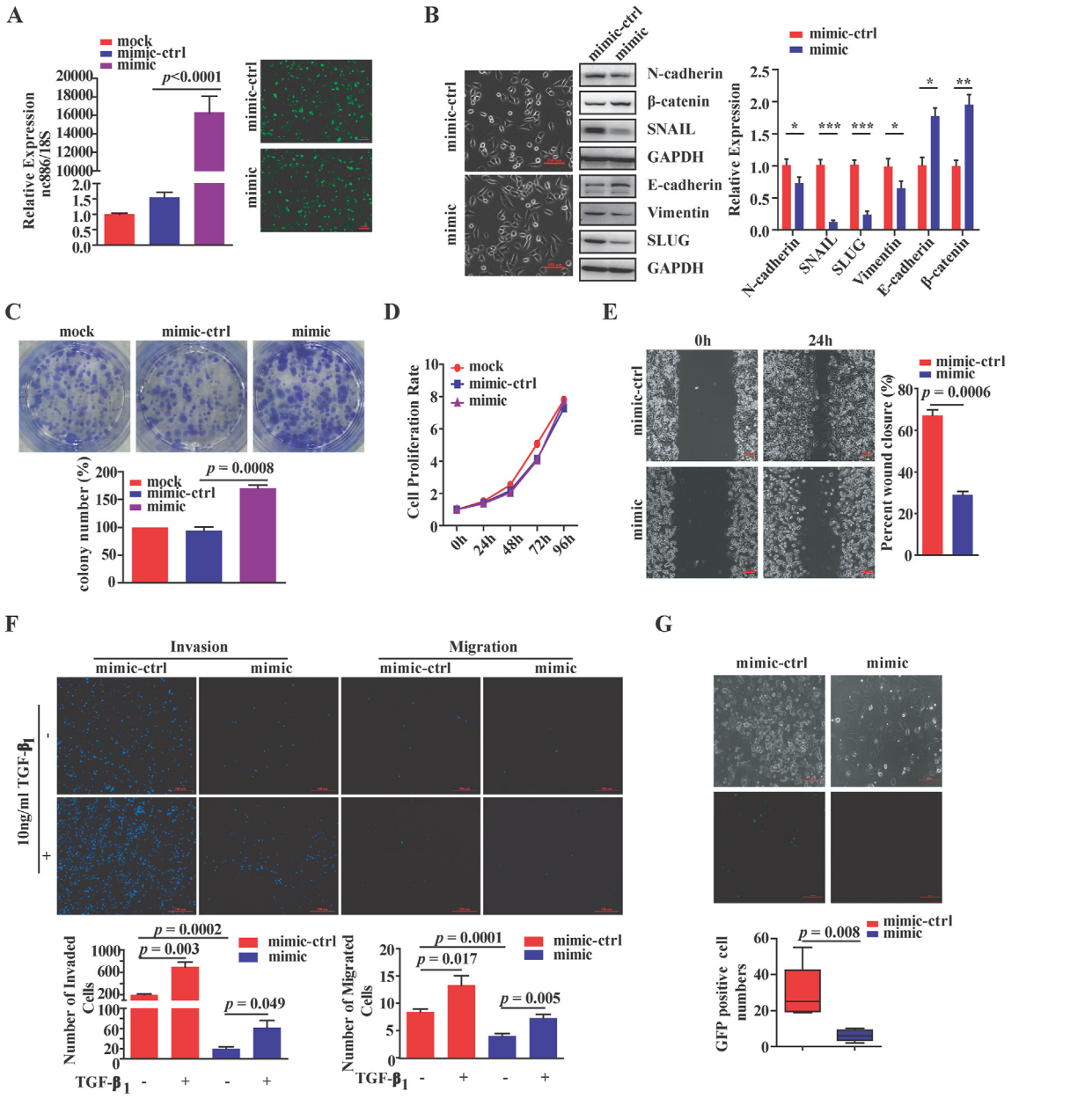

Figure 2 *Nc886* reverses EMT features and decreases PC cell invasion and metastasis *in vitro* and *in vivo*. *In vivo*, we injected 1×10^5 cancer cells into the left ventricles of BALB/c nude mice to investigate the differences between mimic and control cells in distant metastatic ability after 28 days. **(A)** Construction of the 1E8 cell model with stable overexpression of nc886. Cells transfected with GFP plasmid were evaluated using real-time PCR and GFP imaging. **(B)** Comparison of the cell morphology and changes in EMT markers between mimic cell lines and the negative control ($N = 3$). Statistics plot for Western blots are shown. **(C)** Colony formation experiments were performed on mimic cell lines, untreated cells or the negative control ($N = 6$). **(D)** Stably transfected cells ($N = 6$) were checked for cell proliferation using the CCK8 assay. **(E)** Nc886 decreased the wound healing ability of 1E8 cells in scratch assays ($N = 6$). **(F)** Transwell invasion was performed using mimic cell lines or the negative control ($N = 6$) with or without 10 ng/mL TGF-β1 treatment. **(G)** Representative cell light-microscopy image and statistical plot from a BM aspirate after culturing in DMEM for 1 week showing increased highly heterogeneous cell populations in the control group compared to the mimic. We also detected GFP-positive cancer cells in the control group but not in the mimic group. Error bars represent the SD, and an unpaired *t*-test (2-tailed) was used. $^*P < 0.05$; $^{**}P < 0.01$; and $^{***}P < 0.001$.

persistently activated TGFBI at the mRNA levels in the 6 cell lines (Fig. 4H) and temporarily phosphorylated the SMAD5 protein in a time-dependent manner (Fig. 4G), which was inconsistent with the mRNA level data. These data demonstrate that *nc886*, TGFBI and SMAD5 are three independent TGF-β1 targets that are inhibited or activated by TGF-β1 in different manners. TGFBI and SMAD5 activation are key events in TGF-β1-promoted EMT in PC cells. However, the differential regulation mechanism for TGF-β-induced neighboring genes was not elucidated.

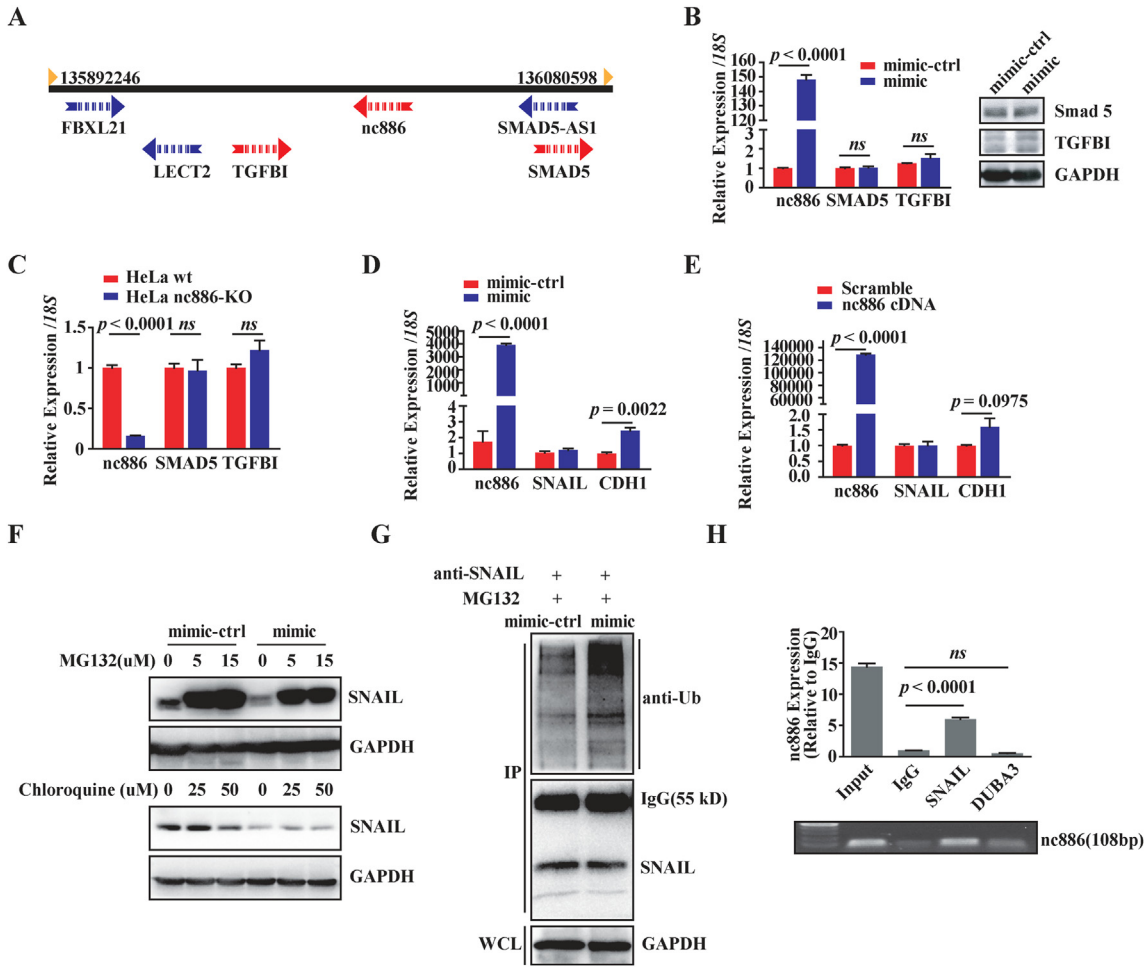

Figure 3 *Nc886* promotes MET in 1E8 cells by directing the targeting of SNAIL protein but not TGFBI or SMAD5. **(A)** Genome diagram illustrating *nc886* adjacent to these two key genes: *TGFBI* and *SMAD5*. **(B)** RT-qPCR was used to examine the mRNA changes in *nc886*, *TGFBI* or *SMAD5*, and Western blotting was used to measure the protein level changes in mimic cells and the negative control. **(C)** We performed only an mRNA-level analysis using RT-qPCR due to growth and passage limits of nc886^{KO} HeLa cells using CRISPR-Cas9 techniques. **(D)** RT-qPCR was used to examine changes in *SNAIL* and *CDH1* mRNA levels in mimic cells or under transient transfection with the nc886 mimic for 24 h in 1E8 cells **(E)**. **(F)** Western blot results showing changes in the levels of SNAIL protein in mimic cells and control cells treated with 15 μM MG132 or different concentrations of chloroquine for 6 h. **(G)** Mimic or control vector cells were treated with MG132 for 12 h. An anti-SNAIL antibody was used to immunoprecipitate endogenous SNAIL protein. Its ubiquitination level was examined using anti-ubiquitin, SNAIL and GAPDH antibodies. **(H)** RT-qPCR detection of *nc886* levels from RNP immunoprecipitation complexes with anti-DUBA3, SNAIL or mouse IgG, and the input. Agarose gel electrophoresis is shown. Error bars represent the SD, and an unpaired *t*-test (2-tailed) was used.

TGF-β1 does not change *TGFBI* or *nc886* promoter methylation levels or the DNMT protein level

Pyrosequencing data confirmed that TGFBI promoter hypermethylation negatively correlated with its expression and caused its expression to be silenced in the 6 cell lines (Fig. 5A, S4A). We verified this result for TGFBI at the protein level using ELISA in the 6 cell lines (Fig. 5B). We found a similar negative correlation between TGFBI promoter hypermethylation and its expression level ($r = -0.149$, $P = 0.001$) in the TCGA-PRAD cohort with a clinical T-value ($N = 490$, Fig. S3). We subsequently measured the changes in the methylation levels of *TGFBI* and *nc886* with TGF-β1 treatment for 24 h in 2B4 and T24 cells, which exhibit low *nc886* and *TGFBI* expression (Fig. 5C, D). Notably, the methylation levels of *TGFBI* or *nc886* in TGF-β1-treated cells were not decreased compared with untreated cells (Fig. 5C, D, S4C). Three active DNA methyltransferases (DNMTs) methylate approximately 70—80% of CpGs in mammals.[31] We also found that two DNMT protein levels showed no changes in T24 and 2B4 cells after TGF-β1 treatment at different time-points using Western blotting (Fig. 5E left). Three DNMT protein levels also showed no changes in 1E8^{nc886+} cells with 10 ng/mL TGF-β1 stimulation for 24 h (Fig. 5E right), which suggests that *nc886* is not correlated with DNMTs. These results suggest that promoter methylation levels do not affect changes in *nc886* and TGFBI expression. Why promoter

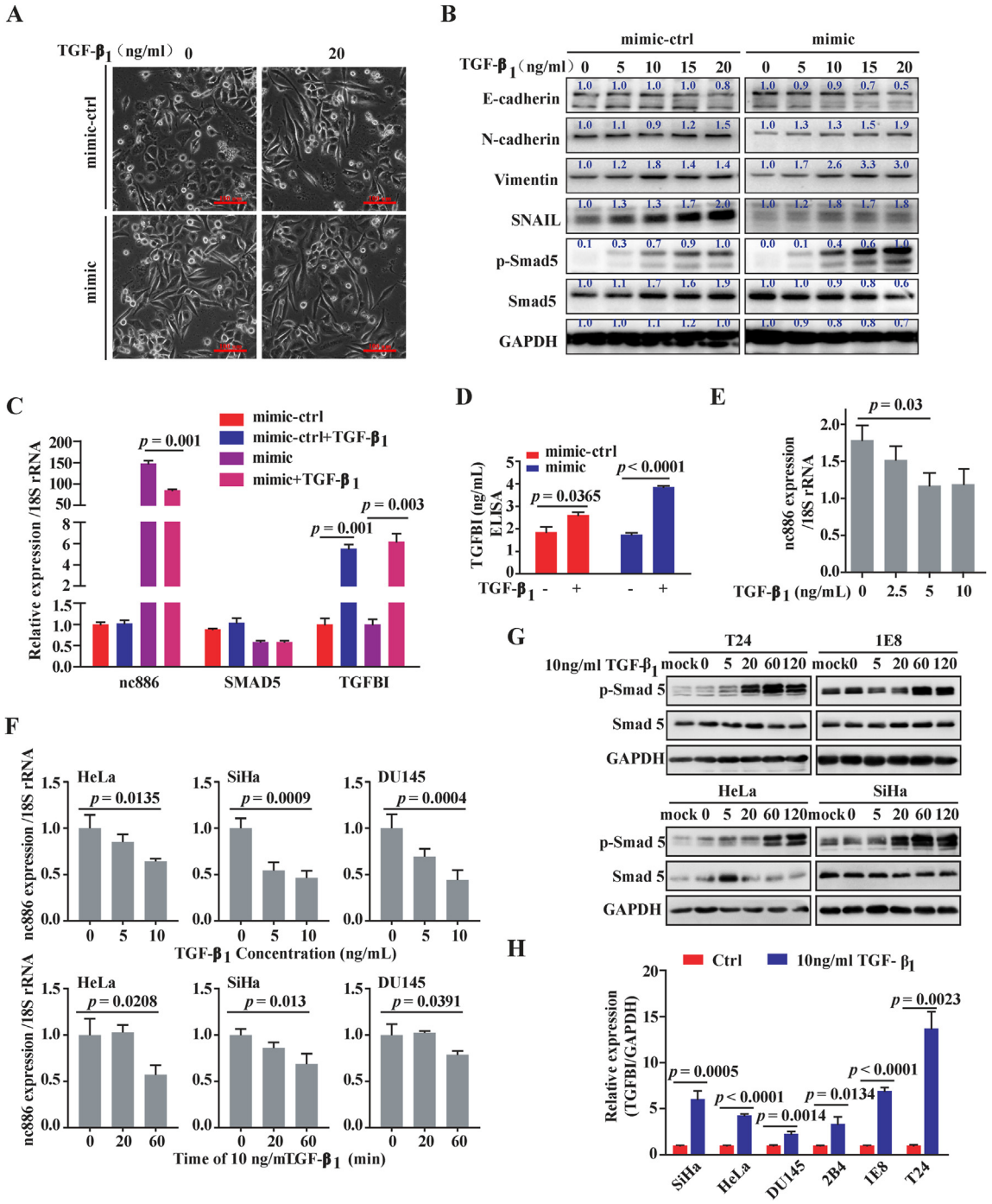

Figure 4 The expression changes of *nc886*, TGFBI and SMAD5 after TGF-β1 treatment in PC cells. **(A, B)** High concentrations of TGF-β1 promote EMT in mimic and control cells. Representative images showing TGF-β1 signal-mediated EMT, and Western blots analyzing changes in known EMT marker (blots and images representative of three independent experiments) in mimic and control cells. **(C)** RT-qPCR detection of changes in *nc886*, *SMAD5* or *TGFBI* mRNA after TGF-β1 treatment for 2 h. **(D)** ELISA was used to examine TGFBI protein activation after TGF-β1 (10 ng/mL) treatment for 24 h. **(E)** TGF-β1 treatment for 1 h reduced the nc886 expression level in a concentration-dependent manner in mimic cells. **(F)** TGF-β1 treatment also transiently reduced nc886 levels in a time- or concentration-dependent manner in other nc886-positive cells, such as SiHa, HeLa or Du145 cells. **(G)** TGF-β1 treatment transiently activated SMAD5 via phosphorylation in the 5-cell line. **(H)** TGF-β1 treatment for 24 h increased *TGFBI* level as assessed using RT-qPCR.

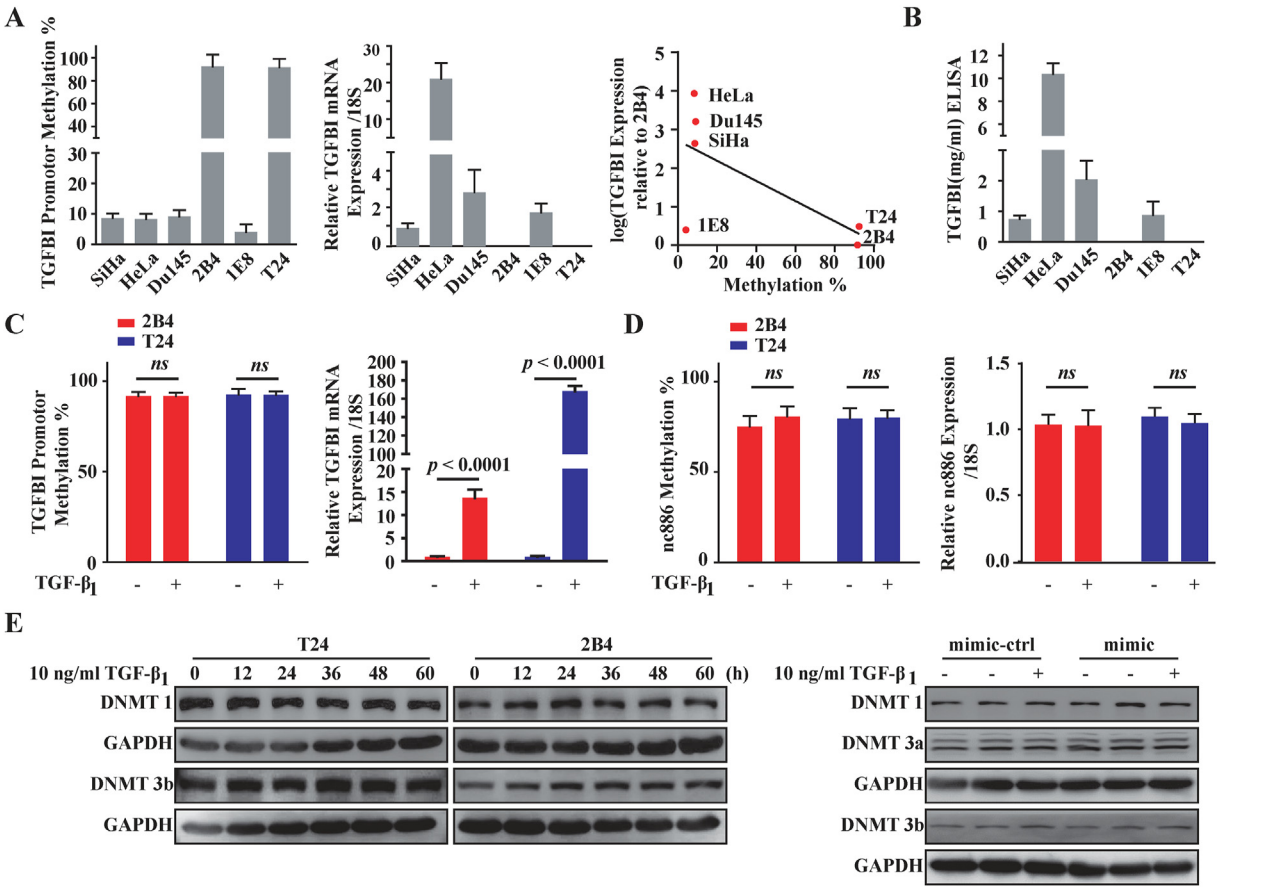

Figure 5 *Nc886* inhibition or TGFBI activation by TGF-β1 is not associated with promoter methylation. **(A)** Quality plot for TGFBI average promoter methylation (in a total of 11 CpGs) or mRNA or protein **(B)** in the 6 cell lines and the negative correlation between the methylation and expression in *TGFBI*. **(C, D)** Plot for *TGFBI* and *nc886* average promoter methylation and expression after treatment of 2B4 and T24 cells with 10 ng/mL TGF-β1 for 24 h, as obtained by pyrosequencing or RT-qPCR, are shown. **(E)** Western blotting was used to analyze the changes in DNMT protein expression in T24 and 2B4 cells and mimic and control cells after TGF-β1 treatment.

hypermethylation did not prevent TGF-β1 stimulation-induced activation of TGFBI at the mRNA level is not known.

TGF-β1 alters the DNA-binding activity of MAZ within *TGFBI* promoters

The GeneCards database revealed a common transcription factor (TF), named MAZ, within the promoters of *nc886*, *TGFBI* and *CDH1* (Fig. 6A). We examined differences in the DNA-binding activity of Pol II and Pol II-associated MAZ after TGF-β1 treatment using ChIP experiments. Three representative PC cell models were selected: 1E8 cells, for high expression of TGFBI and no expression of nc886; 2B4, for negative expression of nc886 and TGFBI; and Du145, for high expression of TGFBI and nc886. A negative control was performed with IgG, and the positive control used Pol II. Our ChIP PCR detected the binding of MAZ to the *TGFBI* promoter only in 2B4 cells (red square indicated in Fig. 6B and red tick in Fig. 6C), and MAZ bound to the *CDH1* promoter in all three cell lines. MAZ did not bind to the GA box of the first exon region in *TGFBI* or *CDH1*. MAZ also did not bind to the A or B promoter region of *nc886* (Fig. 6B, C) in any of the three cell lines. TGF-β1 stimulation for 24 h in 2B4 cells decreased the DNA-binding activity of MAZ on the TGFBI promoter for transcription initiation (Fig. 6D), which suggests that TGF-β1 regulates MAZ and serves as a transcriptional suppressor for the TGFBI promoter region in PC cells. However, MAZ does not act as a transcriptional suppressor for the Pol III-transcribed *nc886* promoter.

Discussion

Our previous findings *in vivo* established that the core change of *nc886* down-regulation of TGF-β1 caused differences in cellular immune rejection in an immunocompetent mouse model.[17] Therefore, we investigated whether TGF-β1-mediated EMT was an important mechanism of *nc886* reduction of prostate cancer cell aggressiveness. Our present study demonstrated that the epigenetic silencing of *nc886* in metastatic samples better correlated with certain EMT markers, such as *CDH1*, *CDH2* and *CTNNB1*, in PC. We established a putative association of *nc886* and certain EMT molecules with PC progression and EMT change based on clinical data from the GEO analysis shown in Figure S2. PC progression from the GS $\leq$ 7 to GS $\geq$ 8 stage involves the process of EMT

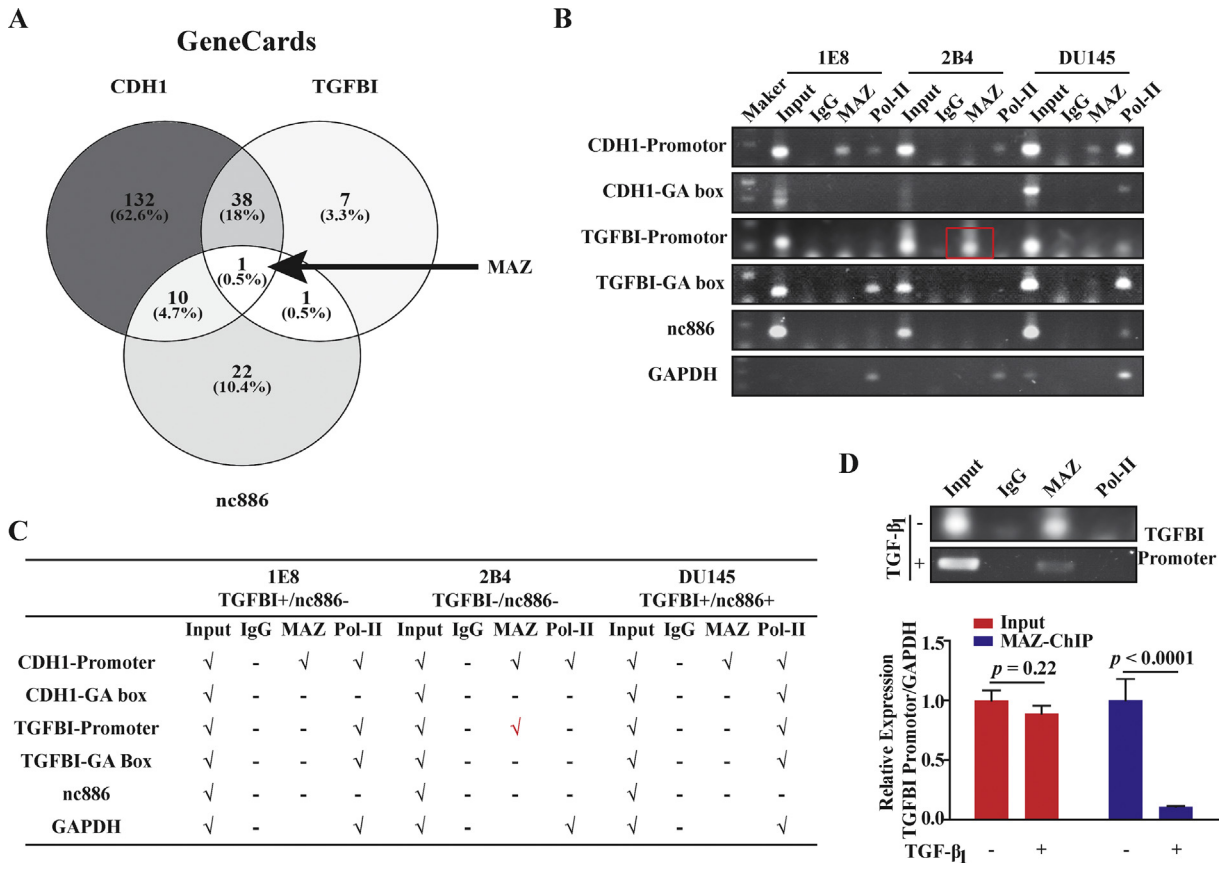

Figure 6 The mechanism of TGF-β1 activation of TGFBI may involve modulation of the ability of MAZ to bind to the TGFBI promoter region. **(A)** Vein graph showing the common TFs in the *CDH1*, *TGFBI* and *nc886* promoters from the GeneCards cohort. **(B)** ChIP experiments investigating MAZ binding to CDH1 promoter, CDH1-GA box, TGFBI-promoter, TGFBI-GA box, nc886 and positive control GAPDH. **(C)** Summary of the ChIP results for stable expression in three PC cell lines with differential expression of nc886 or TGFBI. √ indicates success in PCR, - indicates failure in PCR, and red highlights the tick. **(D)** TGF-β1 decreased MAZ binding to TGFBI promoter in 2B4 cells. Representative images are shown from one of three independent experiments.

induction. GS $\leq$ 7 stage PC exhibits primary or locally invasive tumors, which are endowed with more epithelial characteristics, such as increased *CDH1* or *CDH2*, *nc886* and *CTNNB1* suppression. Cell—cell adhesion is lost at the PC GS $\geq$ 8 stage, in which EMT is induced by *CDH1* suppression or *TGFBI* elevation tendencies. Cancer cells with increased invasive properties break down and invade through the basement membrane and enter the bloodstream in a process called intravasation. These circulating tumor cells (CTCs) subsequently exit the bloodstream to form micro-metastases, which suppress *nc886*, *TGFBI* or *SMAD5*. We found that IE8 cell lines with a high invasive ability exhibited *nc886* and *CDH1* suppression and *TGFBI* elevation, which are similar to clinical GS $\geq$ 8 events (Fig. S2). A good cell model system should reflect *in vivo* events. We selected the 1E8 cell line for an in-depth study of molecular events.

The reintroduction of *nc886* to 1E8 cells reversed their cell mesenchymal behavior, which consists of the formation of epithelial-like cell clusters and increased colony formation, and decreased cell migration and invasion *in vitro* and distant bone metastasis in a nude mouse model. However, the reintroduction of TGF-β1 may reverse this benefit. *Nc886* is an emerging regulator of MET in PC cells. Therefore, we further examined the mechanism.

We first demonstrated that *nc886* failed to alter the expression levels of TGFBI and SMAD5 mRNA and protein, but it promoted SNAIL protein degradation at the post-translational level. RIP experiments established the functional link between *nc886* and SNAIL protein in mimic cell lines. The TF SNAIL, which is the first discovered and well known inducer of EMT,[32] suppresses the transcription of E-cadherin via direct binding to its promoter and promotes EMT in cancer metastasis and progression.[33] Most cellular protein degradation is subject to the ubiquitin-proteasome system control.[34] Increasing evidence highlights a role for UPS control in the regulation of SNAIL activity.[35] The present study demonstrated that *nc886* significantly reduced the expression of SNAIL partially via its promotion of SNAIL ubiquitination, which may explain the negative correlation of *nc886* with *CDH1* in PC samples and cells and the further induction of MET occurrence. *Nc886* may be a good biomarker for PC metastasis due to its role in EMT fine-tuning of PC cells.

However, TGF-β1 treatment suppresses this function of *nc886*. TGF-β1, as the direct targets of hsa-miR-886-3p in small cell lung cancer and PC cell lines,[8,16] was inhibited in mimic cells in our previous study.[17] However, the present study observed that the reintroduction of TGF-β1 temporarily inhibited the transcription of *nc886* but activated the transcription of its neighboring gene *TGFBI* in PC cells, which is consistent with the opposite finding in the advanced ovarian cancer where *nc886* has an oncogenic function.[18] Notably, TGF-β1 stimulation did not change the methylation level in the *nc886* promoter or *TGFBI* and DNMT levels, which suggests that the proteins may be regulated via the same epigenetic mechanism. However, their activation mechanisms are diverse in PC cells. It also suggests a differential regulatory mechanism of gene expression for Pol II and neighboring Pol III genes.

One study revealed that TF-MYC induced *nc886* elevation, even in a hypermethylated state, in breast cancer cell lines.[36] It is well known that MYC and TGF-β1 are mutually inhibited.[37] We observed that *MYC* mRNA showed a 1.5-fold increase in mimic cells with a lower TGF-β1 level than the scramble cells using our previous microarray analysis (GSE143451). TGF-β1-induced MYC downregulation may be a mechanism for that the TGF-β1-induced temporary inhibition of *nc886*. The bioinformatics analysis identified MAZ as a common TF for the promoter regions of *nc886*, *TGFBI* and *CDH1*. MAZ regulates the expression of a variety of genes, for example *c-MYC*.[38–40] Notably, MAZ regulates the transcription or termination of two adjacent genes simultaneously because it binds to the transcriptional terminator region of a upstream gene and the promoter region of the following gene.[41] MAZ also binds to the cis-elements in GC-rich promoters in a position-specific manner[40] and may interrupt the elongation of RNA Pol II and stop transcription.[42] We used *CDH1* as the control to represent a gene distant from *nc886*. The ChIP assay clearly revealed that MAZ was a key target of TGF-β1 differential regulation of *TGFBI* or *nc886* expression. Notably, TGF-β1 increased *TGFBI* mRNA expression via MAZ removal from its promoter, regardless of its methylation status. There is no overlap in promoter regions between *nc886* and *TGFBI*. Although our observation suggests a new mechanism for TGF-β1 differential regulation of the transcription of Pol II and the neighboring Pol III gene, more investigations should be performed in the future. Overall, TGF-β1-induced EMT and *nc886*-promoted MET in PC cells were not two reversible process. TGFBI activation, SMAD5 phosphorylation, *nc886* inhibition and SNAIL overexpression are key events in TGF-β1-induced EMT, but ubiquitinated degradation of SNAIL protein triggered by *nc886* are key events in inversely promoting the initiation of MET. SNAIL is commonly regulated by *nc886* or TGF-β1, but opposite effects exist (Highlight picture).

In conclusion, our findings reinforce the importance of *nc886* in coordinating cell fate, albeit in only 101-nucleotide medium noncoding RNA and Pol III transcripts. The silencing of *nc886* in PC leads to increased distant metastatic ability via the EMT pathway. This silencing represents a negative feedback mechanism for precise

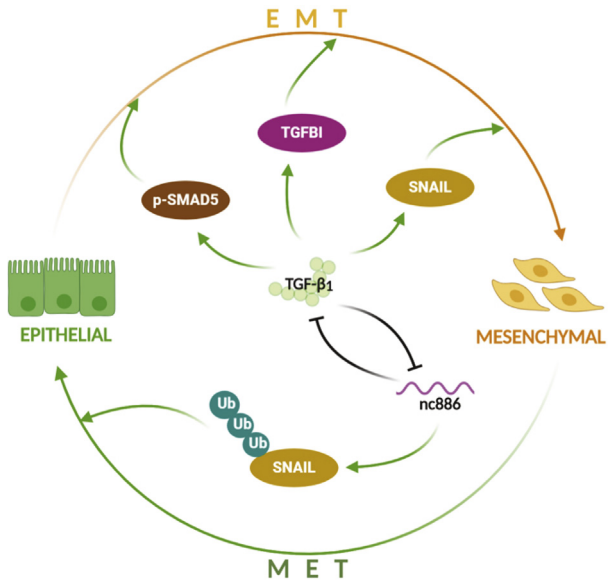

control of the EMT process in PC. However, this feedback loop is disrupted in a TGF-β-enriched tumor microenvironment. TGF-β1 transiently inhibits *nc886* transcription and rapidly promotes the transcription of TGFBI via modulation of the DNA-binding ability of their common TF (MAZ). Therefore, TGF-β1 "kills two birds with one stone."

Author contributions

Concept and design: Lu Kong.
Experimental work: Rong-hui Yang and Ling-kun Zuo and Hui Ma and Ying Zhou.
Analysis and interpretation of data (e.g., pathological diagnosis, statistical analysis, biostatistics, computational analysis): Lu Kong, Li-yong Wang, Ping Zhou, Mahrukh Latif and Miao Wang.
Writing and/or revision of the manuscript: Lu Kong and Mahrukh Latif.

Data availability statement

The data that support the findings of this study are available from the corresponding author upon reasonable request.

Conflict of interests

Authors have no competing interests to declare.

Acknowledgements

The authors thank Ms. Yang Si for her IHC work and a Mapping Website (BioRender.com) in helping to draw

Highlight picture. This work was supported by the Scientific Research Common Program of Beijing Municipal Commission of Education (No. KM202010025004) and the National Nature Science Foundation of China (No. 81672834 and 81272406).

Appendix A. Supplementary data

Supplementary data to this article can be found online at https://doi.org/10.1016/j.gendis.2020.12.010.

Abbreviations

PC	Prostate cancer
ChIP	Chromatin immunoprecipitation
MET	Mesenchymal-to-epithelial transition
EMT	Epithelial-to-mesenchymal transition
DMR	Differentially methylated region
ISH	in situ hybridization
RIP	RNA immunoprecipitation
MAZ	MYC associated zinc finger protein
TGFBI	Transforming growth factor-beta-induced protein
TGF-β	Transforming growth factor-β
DIG	Digoxigenin
GS	Gleason score
TF	Transcription factor

References

1. US Preventive Services Task Force, Grossman DC, Curry SJ, et al. Screening for prostate cancer: US preventive services task force recommendation statement. *JAMA*. 2018;319(18):1901—1913.
2. Song CJ, Chen H, Chen LZ, Ru GM, Guo JJ, Ding QN. The potential of microRNAs as human prostate cancer biomarkers: a meta-analysis of related studies. *J Cell Biochem*. 2018;119(3):2763—2786.
3. Lee YS. A novel type of non-coding RNA, nc886, implicated in tumor sensing and suppression. *Genomics Inform*. 2015;13(2):26—30.
4. Romanelli V, Nakabayashi K, Vizoso M, et al. Variable maternal methylation overlapping the nc886/vtRNA2-1 locus is locked between hypermethylated repeats and is frequently altered in cancer. *Epigenetics*. 2014;9(5):783—790.
5. Kunkeaw N, Jeon SH, Lee K, et al. Cell death/proliferation roles for nc886, a non-coding RNA, in the protein kinase R pathway in cholangiocarcinoma. *Oncogene*. 2013;32(32):3722—3731.
6. Treppendahl MB, Qiu X, Søgaard A, et al. Allelic methylation levels of the noncoding VTRNA2-1 located on chromosome 5q31.1 predict outcome in AML. *Blood*. 2012;119(1):206—216.
7. Lee HS, Lee K, Jang HJ, et al. Epigenetic silencing of the non-coding RNA nc886 provokes oncogenes during human esophageal tumorigenesis. *Oncotarget*. 2014;5(11):3472—3481.
8. Cao J, Song Y, Bi N, et al. DNA methylation-mediated repression of miR-886-3p predicts poor outcome of human small cell lung cancer. *Cancer Res*. 2013;73(11):3326—3335.
9. Calderon BM, Conn GL. Human noncoding RNA 886 (nc886) adopts two structurally distinct conformers that are functionally opposing regulators of PKR. *RNA*. 2017;23(4):557—566.
10. Lee EK, Hong SH, Shin S, et al. nc886, a non-coding RNA and suppressor of PKR, exerts an oncogenic function in thyroid cancer. *Oncotarget*. 2016;7(46):75000—75012.
11. Lei J, Xiao JH, Zhang SH, et al. Non-coding RNA 886 promotes renal cell carcinoma growth and metastasis through the Janus kinase 2/signal transducer and activator of transcription 3 signaling pathway. *Mol Med Rep*. 2017;16(4):4273—4278.
12. Hu Z, Zhang H, Tang L, Lou M, Geng Y. Silencing nc886, a non-coding RNA, induces apoptosis of human endometrial cancer cells-1A in vitro. *Med Sci Monit*. 2017;23:1317—1324.
13. Khoshnevisan A, Parvin M, Ghorbanmehr N, et al. A significant upregulation of miR-886-5p in high grade and invasive bladder tumors. *Urol J*. 2015;12(3):2160—2164.
14. Kong L, Hao Q, Wang Y, Zhou P, Zou B, Zhang YX. Regulation of p53 expression and apoptosis by vault RNA2-1-5p in cervical cancer cells. *Oncotarget*. 2015;6(29):28371—28388.
15. Fort RS, Matho C, Geraldo MV, et al. Nc886 is epigenetically repressed in prostate cancer and acts as a tumor suppressor through the inhibition of cell growth. *BMC Cancer*. 2018;18(1):127.
16. Fort RS, Garat B, Sotelo-Silveira JR, Duhagon MA. vtRNA2-1/nc886 produces a small RNA that contributes to its tumor suppression action through the microRNA pathway in prostate cancer. *Noncoding RNA*. 2020;6(1):7.
17. Ma H, Wang M, Zhou Y, et al. Noncoding RNA 886 alleviates tumor cellular immunological rejection in host C57BL/C mice. *Cancer Med*. 2020;9(14):5258—5271.
18. Ahn JH, Lee HS, Lee JS, et al. nc886 is induced by TGF-beta and suppresses the microRNA pathway in ovarian cancer. *Nat Commun*. 2018;9(1):1166.
19. Cai Q, Chen Y, Zhang D, et al. Loss of epithelial AR increase castration resistant stem-like prostate cancer cells and promotes cancer metastasis via TGF-beta1/EMT pathway. *Transl Androl Urol*. 2020;9(3):1013—1027.
20. Paolillo M, Schinelli S. Extracellular matrix alterations in metastatic processes. *Int J Mol Sci*. 2019;20(19):4947.
21. Moradi Monfared M, Alizadeh Zarei M, Rafiei Dehbidi G, Behzad Behbahani A, Arabsolghar R, Takhshid MA. NDRG2 regulates the expression of genes involved in epithelial mesenchymal transition of prostate cancer cells. *Iran J Med Sci*. 2019;44(2):118—126.
22. Serrano-Gomez SJ, Maziveyi M, Alahari SK. Regulation of epithelial-mesenchymal transition through epigenetic and post-translational modifications. *Mol Cancer*. 2016;15:18.
23. Singh M, Yelle N, Venugopal C, Singh SK. EMT: mechanisms and therapeutic implications. *Pharmacol Ther*. 2018;182:80—94.
24. Chen WY, Tsai YC, Yeh HL, et al. Loss of SPDEF and gain of TGFBI activity after androgen deprivation therapy promote EMT and bone metastasis of prostate cancer. *Sci Signal*. 2017;10(492):eaam6826.
25. Shah JN, Shao G, Hei TK, Zhao Y. Methylation screening of the TGFBI promoter in human lung and prostate cancer by methylation-specific PCR. *BMC Cancer*. 2008;8:284.
26. Li LC, Carroll PR, Dahiya R. Epigenetic changes in prostate cancer: implication for diagnosis and treatment. *J Natl Cancer Inst*. 2005;97(2):103—115.
27. Pan YB, Zhang CH, Wang SQ, et al. Transforming growth factor beta induced (TGFBI) is a potential signature gene for mesenchymal subtype high-grade glioma. *J Neurooncol*. 2018;137(2):395—407.
28. Ramachandran A, Vizán P, Das D, et al. TGF-beta uses a novel mode of receptor activation to phosphorylate SMAD1/5 and induce epithelial-to-mesenchymal transition. *Elife*. 2018;7:e31756.
29. Toth AM, Devaux P, Cattaneo R, Samuel CE. Protein kinase PKR mediates the apoptosis induction and growth restriction phenotypes of C protein-deficient measles virus. *J Virol*. 2009;83(2):961—968.
30. Lee YS, Kunkeaw N, Lee YS. Protein kinase R and its cellular regulators in cancer: an active player or a surveillant? *Wiley Interdiscip Rev RNA*. 2020;11(2):e1558.
31. Sharma S, De Carvalho DD, Jeong S, Jones PA, Liang G. Nucleosomes containing methylated DNA stabilize DNA

methyltransferases 3A/3B and ensure faithful epigenetic inheritance. *PLoS Genet*. 2011;7(2):e1001286.
32. Meindl-Beinker NM, Dooley S. Transforming growth factor-beta and hepatocyte transdifferentiation in liver fibrogenesis. *J Gastroenterol Hepatol*. 2008;23(Suppl 1):S122—S127.
33. Ji Q, Liu X, Han Z, et al. Resveratrol suppresses epithelial-to-mesenchymal transition in colorectal cancer through TGF-beta1/Smads signaling pathway mediated Snail/E-cadherin expression. *BMC Cancer*. 2015;15:97.
34. Guerriero JL, Sotayo A, Ponichtera HE, et al. Class IIa HDAC inhibition reduces breast tumours and metastases through anti-tumour macrophages. *Nature*. 2017;543(7645):428—432.
35. Zhu R, Liu Y, Zhou H, et al. Deubiquitinating enzyme PSMD14 promotes tumor metastasis through stabilizing SNAIL in human esophageal squamous cell carcinoma. *Cancer Lett*. 2018;418:125—134.
36. Park JL, Lee YS, Kunkeaw N, Kim SY, Kim IH, Lee YS. Epigenetic regulation of noncoding RNA transcription by mammalian RNA polymerase III. *Epigenomics*. 2017;9(2):171—187.
37. Smith AP, Verrecchia A, Fagà G, et al. A positive role for Myc in TGFbeta-induced Snail transcription and epithelial-to-mesenchymal transition. *Oncogene*. 2009;28(3):422—430.
38. Medina-Martinez O, Haller M, Rosenfeld JA, O'Neill MA, Lamb DJ, Jamrich M. The transcription factor Maz is essential for normal eye development. *Dis Model Mech*. 2020;13(8):dmm044412.
39. Yu ZH, Lun SM, He R, et al. Dual function of MAZ mediated by FOXF2 in basal-like breast cancer: promotion of proliferation and suppression of progression. *Cancer Lett*. 2017;402:142—152.
40. Álvaro-Blanco J, Urso K, Chiodo Y, et al. MAZ induces MYB expression during the exit from quiescence via the E2F site in the MYB promoter. *Nucleic Acids Res*. 2017;45(17):9960—9975.
41. Kumar P, Yadav VK, Baral A, Kumar P, Saha D, Chowdhury S. Zinc-finger transcription factors are associated with guanine quadruplex motifs in human, chimpanzee, mouse and rat promoters genome-wide. *Nucleic Acids Res*. 2011;39(18):8005—8016.
42. Bossone SA, Asselin C, Patel AJ, Marcu KB. MAZ, a zinc finger protein, binds to c-MYC and C2 gene sequences regulating transcriptional initiation and termination. *Proc Natl Acad Sci U S A*. 1992;89(16):7452—7456.